Published in final edited form as:

J Trace Elem Med Biol. 2020 January ; 57: 21–27. doi:10.1016/j.jtemb.2019.09.001.

The role of poly(ADP-ribose) polymerases in manganese exposed Caenorhabditis elegans

Catherine Neumann[a], **Jessica Baesler**[a,b], **Gereon Steffen**[a], **Merle Marie Nicolai**[a,e], **Tabea Zubel**[c], **Michael Aschner**[d], **Alexander Bürkle**[c], **Aswin Mangerich**[c], **Tanja Schwerdtle**[a,b], **Julia Bornhorst**[*,a,b,e]

[a]Department of Food Chemistry, Institute of Nutritional Science, University of Potsdam, Arthur-Scheunert-Allee 114-116, 14558 Nuthetal, Germany

[b]TraceAge – DFG Research Unit FOR 2558, Berlin-Potsdam-Jena, Germany

[c]Department of Biology, University of Konstanz, Universitaetsstraße 10, 78464 Konstanz, Germany

[d]Department of Molecular Pharmacology, Neuroscience, and Pediatrics, Albert Einstein College of Medicine, 1300 Morris Park Avenue, 10461 Bronx, NY, USA

[e]Food Chemistry, Faculty of Mathematics and Natural Sciences, University of Wuppertal, Gaußstraße 20, 42119 Wuppertal, Germany

Abstract

Background and Aim: When exceeding the homeostatic range, manganese (Mn) might cause neurotoxicity, characteristic of the pathophysiology of several neurological diseases. Although the underlying mechanism of its neurotoxicity remains unclear, Mn-induced oxidative stress contributes to disease etiology. DNA damage caused by oxidative stress may further trigger dysregulation of DNA-damage-induced poly(ADP-ribosyl)ation (PARylation), which is of central importance especially for neuronal homeostasis. Accordingly, this study was designed to assess in the genetically traceable *in vivo* model *Caenorhabditis elegans* the role of PARylation as well as the consequences of loss of pme-1 or pme-2 (orthologues of PARP1 and PARP2) in Mn-induced toxicity.

Methods: A specific and sensitive isotope-dilution liquid chromatography-tandem mass spectrometry (LC-MS/MS) method was developed to quantify PARylation in worms. Next to monitoring the PAR level, pme-1 and pme-2 gene expression as well as Mn-induced oxidative stress was studied in wildtype worms and the pme deletion mutants.

Results and Conclusion: While Mn failed to induce PARylation in wildtype worms, toxic doses of Mn led to PAR-induction in pme-1-deficient worms, due to an increased gene expression of pme-2 in the pme-1 deletion mutants. However, this effect could not be observed at sub-toxic Mn doses as well as upon longer incubation times. Regarding Mn-induced oxidative stress, the

[*]Corresponding author address: Food Chemistry, Faculty of Mathematics and Natural Sciences, University of Wuppertal, Gaußstrasse 20, 42119 Wuppertal, Germany Tel. ++49 202 439-3453 Fax ++49 202 439-3073, bornhorst@uni-wuppertal.de.

Conflicts of interest

The authors declare no conflict of interest.

deletion mutants did not show hypersensitivity. Taken together, this study characterizes worms to model PAR inhibition and addresses the consequences for Mn-induced oxidative stress in genetically manipulated worms.

Graphical abstract

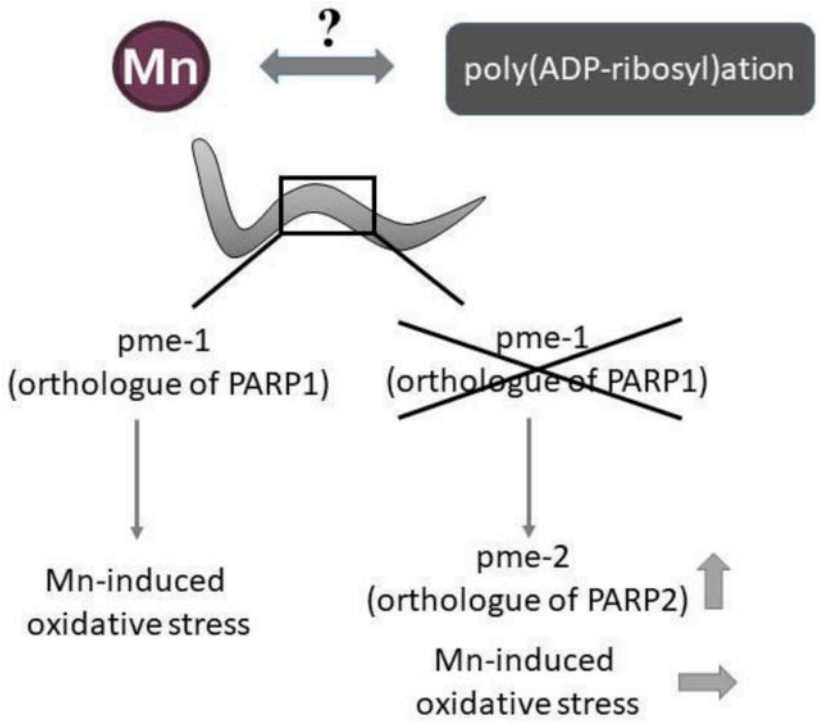

Keywords

Manganese; Caenorhabditis elegans; oxidative stress; DNA damage response; poly(ADP-ribosyl)ation

Introduction

Metal ions, such as mercury, lead, manganese, copper, iron, aluminum, bismuth, thallium and zinc play crucial roles in the complex multi-factorial mechanisms of neurodegenerative diseases (summarized in [1]). Excessive and prolonged exposure to the plentiful of the naturally occurring trace element manganese (Mn) has been documented to cause neurological impairment which is termed “manganism”. The motor and cognitive deficits are similar to those observed in idiopathic Parkinson’s disease (PD) [2, 3]. Differences from PD include the lack of nigrostriatal dopaminergic neuron damage and the classic response to levodopa [4]. However, Mn exposure is further supposed to be a risk factor for the development of PD [5]. In earlier studies Mn neurotoxicity has been described clinically in workers exposed occupationally to high Mn levels, but the exposure scenarios changed during the last century from acute to chronic low-level environmental and/or occupational exposure [3, 6]. Concerns are mounting about adverse neurological effects in children, since Mn overexposure may result in lower IQ scores, changes in cognitive abilities, as well as

altered short-term memory and motor control [7, 8]. To date the molecular mechanisms behind Mn induced neurotoxic effects remain unclear. It has been attributed to alterations in a variety of cellular functions including disruptive effects on the neurochemistry of neurotransmitters or oxidative stress [2, 9]. Taking oxidative stress into account, excessive reactive oxygen and nitrogen species (RONS) formation leads to increase of interactions with macromolecules such as the DNA. Recently, we identified the DNA damage related signaling reaction poly(ADP-ribosyl)ation (PARylation) to be highly sensitive to *in vitro* Mn exposure, corroborating the sensitization of cells to genotoxic treatment [10, 11].

PARylation is a posttranslational modification of proteins, which is associated with numerous cellular processes such as DNA repair, protein turnover, inflammation, aging or metabolic regulation [12, 13]. Poly(ADP-ribose) polymerase-1 (PARP1) and poly(ADP-ribose) polymerase-2 (PARP2) are localized in the nucleus and both of them participate in the early DNA damage response. Thereby the catalytic activity of PARP1 is stimulated 500-fold by DNA with single-strand or double-strand DNA breaks. Although, the basal level of ADP-ribosylation is relatively low, PARPs can consume up to 90% of cellular NAD^+ upon DNA damage attaching ADP-ribose moieties onto various acceptor proteins or PARP1 itself [14]. Consequently, over-activation as well as inhibition of PARP1 or PARP2 does have severe consequences [12, 13, 15]. Although PARP1 inhibitors have excelled in targeting cancers, its beneficial application in neurodegenerative settings has been controversial [16, 17]. On one hand, it is used as therapeutic option for stroke in clinical trials [16]. On the other hand, PARP1 inhibition diminishes mitochondrial capacity and rate of DNA repair with severe consequences for neuronal cells as cell death [16]. Additionally, since PARP1 activation has been associated with neurite outgrowth and long-term memory [18, 19], it is conceivable that chronic PARP1 inhibition may attenuate neurogenesis and learning. Considering the importance of PAR homeostasis as well as findings showing that elevated dietary Mn exposure may cause neurobehavioral and neurocognitive deficits in children [20–22], the role of the DNA damage response in Mn-induced toxicity merits further investigation.

The simplicity and several key features of the nematode *Caenorhabditis elegans* (*C. elegans*) turned it into an appealing model organism to study the role of PAR in Mn-induced toxicity *in vivo*. Characteristics that have been contributed to its success include among others the genetic manipulability, the well-characterized genome and the ease of maintenance. The nematode is less complex than a mammalian system, while still sharing considerable genetic homology (60 – 80%) [23].

Material and methods

C. elegans strains, Mn treatment and Mn-induced lethality assay

The *C. elegans* strains were handled and maintained at 20 °C as previously described [24]. The following strains were used in this study: WT N2 Bristol strain, OH7193 (otIs181 [P_{dat-1}::mCherry + P_{ttx-3}::mCherry] III.; him-8(e1489) IV.) and the deletion mutants RB1042 (parp-1(ok988) I.) and VC1171 (parp-2(ok344) II.). All strains were provided by the Caenorhabditis Genetic Center (CGC; University of Minnesota).

Synchronous L1 populations were placed on OP50-seeded NGM plates after hatching and experiments were performed using L4 stage nematodes [25]. The L4 stage nematodes were exposed to $MnCl_2$ solution in siliconized tubes for 1 h or 4 h in 85 mM NaCl containing 0.01% Tween. $MnCl_2$ (>99.995% purity) (Sigma-Aldrich) stock solutions were prepared in 85 mM NaCl. After treatment, worms were washed at least three times with 85 mM NaCl containing 0.01% Tween and subjected to further analyses as described below.

For lethality testing the worms were transferred to OP50-seeded NGM plates and dead worms were manually counted 24 h post treatment.

Analysis of poly(ADP-ribosyl)ation (PAR) levels

For PAR extraction, worm pellets were prepared from 6,000 L4 worms exposed to $MnCl_2$. This was followed by washing the worms three times with 85 mM NaCl containing 0.01% Tween, five times freeze and thaw cycles in liquid nitrogen and homogenizing with a tissue disruptor (Qiagen) in 1 mL ice-cold 20% TCA (w/v). The sample preparation was performed as previously described [26, 27] with some adaptations. Briefly, the precipitate was centrifuged at 3,000 × *g* and 4°C for 10 min, washed twice with ice-cold 70% EtOH and air-dried at 37°C. Thereafter, the pellets were resuspended in 400 µL 0.5 M KOH to detach protein-bound PAR and incubated at 37°C for 50 min. The cell debris was pelleted and the supernatant neutralized with 4.8 M MOPS (pH 5.9), and 30 µL aliquots were used to determine the DNA concentration for normalization. Modifications of the previously described Hoechst method [26, 27] include that the standard solutions and samples were incubated for 5 min with 0.5 µg/mL Hoechst 33342 (Molecular Probes) and subsequently transferred into a 384-well plate in duplicates. The fluorescence was monitored (excitation 355 nm/emission 460 nm) with a microplate reader (Tecan Infinite M200 Pro).

2.5 pmol of $^{13}C,^{15}N$ labeled-PAR were added to the supernatant (the *in vitro* synthesis of PAR was carried out as described in [27]). To digest nucleic acids, i.e., DNA and RNA, add 6.25 µL 2-M $MgCl_2$, 2.5 µL 100-mM $CaCl_2$, 12.5 µL 2-mg/ml DNase and 2.5 µL 10-mg/ml RNase and incubate at 37°C for 3 h, following digestion with 1.25 µL 40 mg/mL proteinase K (Roche) overnight. After enriching samples for PAR by the High Pure miRNA isolation kit (Roche) and digesting to its monomeric units with an alkaline phosphatase from bovine intestine mucosa (AP) (Sigma-Aldrich) and phosphodiesterase I (PDE) (Affymetrix), enzymes were removed with a 10 kDa cut-off filter (Nanosep 10K, Pall). The vacuum-dried and in water resuspended sample was subjected to LC-MS/MS analysis.

The PAR analyses were conducted with an Agilent 1260 Infinity LC system coupled to an Agilent 6490 triple quadrupole-mass spectrometer (both from Waldbronn, Germany) equipped with an electrospray ion source operating in the positive ion mode (ESI+). Analyte separation was carried out using a Hypersil Gold aQ 150 × 2.1 mm particle size 3 micron (Thermo Scientific). Water and acetonitrile (Roth), both acidified with 0.1% formic acid, were used as eluents. Compounds were separated isocratically with 1% acidified acetonitrile at a flow rate of 0.3 mL/min. The following ion source parameters were determined after repeated injection of a PAR standard solution using the *Source Optimizer* tool of the Agilent MassHunter Workstation Software (Version B.06.00): drying gas temperature = 260 °C, drying gas flow = 11 L min^{-1} of nitrogen, sheath gas temperature = 380 °C, sheath gas flow

= 12 L min^{-1} of nitrogen, nebulizer pressure = 40 psi, capillary voltage = 4000 V, nozzle voltage = 0 V. The optimized ion funnel parameters were: high pressure RF voltage = 190 V and low pressure RF voltage = 40 V. The optimized collision energies for the MRM transition, which were determined using the *Optimizer* tool of the MassHunter Software, are 25 V for the transitions of *m/z* 400 > 136 and *m/z* 415 > 146 for the quantification of ribosyladenosine (R-Ado) and ^{13}C,^{15}N R-Ado, respectively.

TaqMan gene expression assay

Total RNA was isolated using the Trizol method as published elsewhere [28]. Following isolation, 1 μg total RNA was subjected to cDNA synthesis applying the High Capacity cDNA Reverse Transcription Kit (Applied Biosystems) according to the manufacturer's instructions. Quantitative real-time PCR (BioRad) was conducted using TaqMan Gene Expression Assay probes (Life Technologies). Data were normalized to the housekeeping gene afd-1 (actin homolog) after calculation of the fold change applying the comparative 2-ΔΔCt method. The following probes were used: pme-1 (assay ID: Ce02415136_m1), pme-2 (assay ID: Ce02437339_g1) and afd-1 (assay ID: Ce02414573_m1).

Energy related nucleotides

Worm extracts were prepared using 6,000 L4 stage worms following after Mn exposure. After washing, worms were centrifuged and the supernatant was discarded. Zirconia beads and 150 μL 0.5 M KOH were added to the worm pellet and homogenized exactly 40 s in a Bead Ruptor (Biolabproducts GmbH). The extracts were neutralized by adding 30 μL phosphoric acid (10%) and centrifuged at 20,630 g for 30 minutes (4°C). Immediately thereafter the nucleotides (ATP, ADP, AMP, NAD+, NADH) were measured by ion-pair-reversed-phase-high-performance liquid chromatography with diode-array-detector [29].

Analysis of glutathione equivalents

Total intracellular glutathione levels (reduced and oxidized GSH) were conducted with an Agilent 1260 Infinity LC system coupled to an Agilent 6495 triple quadrupole-mass spectrometer (both from Waldbronn, Germany) interfaced with an electrospray ion source operating in the positive ion mode (ESI+). Worm extracts were prepared out of 3,000 L4 worms exposed to $MnCl_2$. This was followed by washing with 85 mM NaCl and by three cycles of freezing in liquid nitrogen and thawing. After adding Zirconia beads and 300 μL ice-cold extraction buffer (1% Triton X-100, 0.6% sulfosalicylic acid and 1% protease inhibitor in KPE buffer (0.1 M potassium phosphate buffer, 5 mM EDTA)) containing the isotopic labeled internal standard (Glutathion-[glycin-$^{13}C_2$,^{15}N]), worms were homogenized three times 20 s in a Bead Ruptor. After centrifugation, supernatants were used for LC-MS/MS analysis [30]. Three mass transitions each were used for MRM analysis of GSSG and GSH. The most abundant mass transition (quantifier) was chosen for quantification, with additional mass transitions (qualifier) used for unequivocal identification. The MRM transition *m/z* 307 > 130 (collision energy: 9V) was used for quantification of GSSG, *m/z* 308 > 179 (collision energy: 9V) was used for quantification of GSH and *m/z* 311 > 182 (collision energy: 9V) for the internal standard. Concentrations of the glutathione equivalents were normalized to the protein content determined by the bicinchoninic acid (BCA) assay-kit (Thermo Scientific, Schwerte, Germany).

MitoTracker dyes and fluorescence quantification

Whereas MitoTracker Green FM is used to assess mitochondrial mass, MitoTracker Red CM-H_2XRos detects the mitochondrial membrane potential- and mitochondrial-derived RONS (Thermo Fisher Scientific) [31]. L4 worms were incubated with the respective Mitotracker dye in the dark for 2 h (1 μM MitoTracker Green FM; 50 μM MitoTracker Red CM-H_2XRos). Afterwards worms are washed four times with 85 mM NaCl containing 0.01% Tween and next treated with $MnCl_2$ for 1 h. After three washes, worms were placed on OP50-spread NGM plates for 2 h, allowing for excess dye to be excreted. The fluorescence was monitored with a microplate reader (Tecan Infinite M200 Pro) (red: excitation 560 nm/emission 599 nm; green: excitation 485 nm/emission 525 nm). MitoTracker Green FM was carried out in Pdat-1::mCherry + Pttx-3::mCherry worms. Therefore, the OH7193 worms him-8(e1489) were outcrossed and pme-1 as well as pme-2 worms were crossed with the otIs181 [Pdat-1::mCherry + Pttx-3::mCherry] worms (otIs181 [Pdat-1::mCherry + Pttx-3::mCherry] III.; parp-2(ok344) II.; otIs181 [Pdat-1::mCherry + Pttx-3::mCherry] III.; parp-1(ok988) I.). The green fluorescence of the MitoTracker Green FM was normalized to the worm number correcting it for red fluorescence in the worms.

Statistical analysis

Dose-response curves and histograms were generated using GraphPad Prism (GraphPad Software Inc.). All data presented in the figures are mean values + SEM. In order to compare the applied *C. elegans* strains as well as concentrations two-way analysis of variance (ANOVAs) were performed, followed by Tukey's multiple comparisons test. A p-value < 0.05 was considered significant.

Results

Effect of 1 h and 4 h Mn exposure on the survival of *C. elegans*

To assess the effect of Mn toxicity and determine optimal dosing, wildtype (WT) worms as well as the deletion mutants of pme-1 and pme-2 were treated with increasing Mn doses. The dose–response survival curves (Figure 1) show that the genetic deletion of either gene did not increase mortality in L4 worms exposed 1 h or 4 h to Mn, with an LD50 indistinguishable from wildtype (WT) worms for the respective exposure time. 1 h Mn exposure leads to an LD50 of 250 mM (Figure 1A), whereas 4 h exposure resulted in a leftward-shift to an LD50 of 60 mM for all analyzed strains (Figure 1B).

Effects of Mn treatment on poly(ADP-ribosyl)ation (PARylation)

Non-exposed pme-1 deletion mutants exhibited a significant lower basal level of PAR compared to WT worms (Figure 2A and B). However, pme-2 deletion mutants did not show this effect. After 1 h as well as 4 h incubation Mn exerted no effect on PAR induction in WT worms as well as in pme-2 deletion mutants. Interestingly, 250 mM Mn exposure resulted in the pme-1 deletion mutants in a significant PAR-induction compared to the non-exposed pme-1 worms (Figure 2A). Four h Mn exposure did not increase PAR levels in the pme-1 deletion mutants (Figure 2B).

Pme-1 and pme-2 gene expression

In WT worms 1 h as well as 4 h Mn exposure did not affect the gene expression of pme-1 or pme-2 (data not shown). To investigate whether the Mn-induced PAR induction in the pme-1 mutant might contribute to changes in gene expression, we examined the pme-2 expression in the pme-1 deletion mutants (Figure 3) and the pme-1 expression in the pme-2 deletion mutants (Figure 3). Figure 3A clearly show the significant increase of the pme-2 expression in the pme-1 deletion mutants following 1 h Mn exposure. 4 h Mn exposure did not affect the pme-2 expression. Pme-1 expression is unchanged upon 1 h and 4 h Mn exposure compared to non-exposed pme-2 deletion mutants.

Effect on the level of energy related nucleotides

Non-exposed pme-2 deletion mutants bear a lower basal ATP level as compared to WT worms, while NAD^+, NADH (data not shown) and its ratio are indistinguishable from WT worms (Figure 4). Treatment with Mn (250 mM) for 1 h significantly increased the NAD^+ level in all three strains. One-hundred mM Mn exposure further increased the NAD^+ levels in the pme-2 mutants (Figure 4B). A direct comparison of the deletion mutants indicates higher NAD^+ level at 100 mM treatment in the pme-2 mutant. Figure 4C demonstrates increased NAD^+/NADH ratio in the deletion mutants treated with 250 mM Mn. Four h Mn exposure is accompanied with a decreased ATP level in the WT worms. In pme-1 mutants, only the highest dose led to significant changes (Figure 4D). Comparing the NAD^+ level following 60 mM Mn exposure, pme-1 mutants showed lower values as the WT worms (Figure 4E). The corresponding effect can also be observed in the NAD^+/NADH ratio. Additionally, in all strains Mn treatment led to a significant induction of the NAD^+/NADH ratio at the highest dose (60 mM). Interestingly, pme-1 deletion mutants displayed a lower NAD^+/NADH ratio than the WT worms and pme-2 deletion mutants (Figure 4F).

Effect on oxidative stress endpoints

Oxidative stress is implicated in Mn-induced toxicity [28, 32] and increasing RONS level may lead to reactions with macromolecules, such as DNA. One consequence might be the occurrence of DNA strand breaks, which can activate PARP-1. Therefore, we investigated Mn-induced oxidative stress in WT worms and the deletion mutants by means of glutathione (GSH) equivalents, the mitochondrial membrane potential- and mitochondrial-derived RONS, as well as the mitochondrial mass. While upon Mn exposure the GSH level were unchanged (data not shown) in the tested strains, GSSG increased significantly in WT worms and pme-1 deletion mutants after treatment with 250 mM Mn (Figure 5A). Contrary to the pme-1 deletion worms, the pme-2 mutants showed no significant Mn-induced GSSG induction. The GSH/GSSG ratio was reduced in WT worms as well as the deletion mutants following 250 mM Mn exposure (Figure 5B). Figure 5C shows Mn-induced mitochondrial-derived RONS and damage to the mitochondrial membrane potential in WT worms and the pme-1 mutants upon 250 mM Mn treatment. Surprisingly, the genetic deletion of pme-1 or pme-2 resulted in a lower Mn-induced RONS induction compared to the WT worms at the highest dose (Figure 5C). Next, we assessed whether Mn affected the mitochondrial mass. Mn treatment reduced the mitochondrial mass in WT worms and the deletion mutants (Figure 5D).

Discussion

A balanced regulation of the DNA damage response reaction PARylation is of central importance and a dysregulation (inhibition as well as over-activation) is associated with detrimental consequences for several aspects of brain physiology and physiopathology [16]. This implicates the importance of DNA damage response in neural homeostasis. We have recently identified the DNA damage related signaling reaction PARylation to be highly sensitive to *in vitro* Mn exposure [10, 11].

Accordingly, this study was designed to assess the role of the DNA damage response in Mn-induced neurotoxicity *in vivo* with a special focus on interactions of the Poly(ADP-ribose) polymerase 1 and 2 and Mn using the genetically traceable organism *C. elegans*. Although several DNA repair pathways (base excision repair, nucleotide excision repair as well as DSB repair [non-homologous end-joining (NHEJ) and homologous recombination (HR)] occur in the nematode [33–35], only a limited number of studies exist regarding *C. elegans* and DNA damage response, especially PARylation. However, using *C. elegans*, where the number of key players of the DNA damage response and DNA repair pathway is rather restricted, may provide answers to key gaps of many questions raised *in vitro* as well as in mammalian model systems. Gagnon et al. reported in 2002 the presence of the poly(ADP-ribose)metabolism enzyme (pme) in the worm. They identified and characterized pme-1 and pme-2 as structural orthologues of mammalian PARP1 and PARP2, respectively. Functional analysis using ionizing radiation in order to induce PARylation confirmed that pme-1 and pme-2 act in similar roles as their mammalian counterpart [36, 37]. The physiological importance of the DNA damage response was highlighted when worms were incubated with mammalian PARP inhibitors and irradiated [37]. However, PARylation of worm proteins was only qualitatively assessed by Western blot analysis [37]. In order to quantify PAR level in worms with unequivocal chemical specificity in absolute terms with femtomol sensitivity, isotope dilution mass spectrometry (LC-MS/MS) was used in this study [26, 27]. The established method based on the protocol of Zubel et al. (2017) [27] enables the analysis of steady-state levels of PAR in wildtype worms as well as pme-1 and pme-2 deletion mutants. Since the expression of pme-1 and pme-2 genes is developmentally regulated in *C. elegans* [36], L4 larvae were used in this study. The data confirmed the expected lower steady-state PARylation of worm proteins in the pme-1 deletion mutants (Figure 2A and B). This underlines further the suggestion of Mouchiroud et al. (2013) concluding based on their lifespan data exposing worms to the PARP-inhibitor AZD2281 that pme-1 holds the major worm PARP activity [38]. We further confirmed the mammalian PARP2 data that the steady-state PAR was only was slightly reduced in the absence of pme-2 (Figure 2A and B) [39]. In order to ensure that PARylation in the nematode is inducible by the applied method tert-butyl hydroperoxide (t-BOOH) was used as positive control (Supplementary Figure 1). Time and concentration dependent t-BOOH exposure revealed in WT worms the highest PAR-induction incubating 6.5 mM tBOOH for 1 h. Mn exposure did not significantly induce PARylation in wildtype worms as previously observed in *in vitro* studies [10, 11]. Surprisingly, 1 h Mn exposure resulted in a significant PAR-induction in the pme-1 deletion mutants (Figure 2A). This might be due to the induction of the pme-2 gene expression in the pme-1 deletion mutants following 1 h Mn exposure (Figure 3A). However, neither Mn-

induced PARylation nor Mn-induced pme-2 gene expression were observed following 4 h Mn exposure. Being a substrate of PARPs, the maintenance of a NAD^+ pool is of central importance. Quantifying the NAD^+ level indicated in the pme-1 mutants a lower level following 60 mM Mn exposure for 4 h. This might contribute to the absence of Mn-induced PARylation following 4 h 60 mM Mn exposure. While higher level of NAD^+ were observed in the pme-1 mutant worms [38, 40], in our study the pme-1 and pme-2 deletion mutants show an indistinguishable steady-state NAD^+ level to WT worms. 1 h Mn exposure resulted in all strains in an induction of the NAD^+ level which seems to be independent of the Mn-induced PAR-induction only observed in pme-1 deletion mutants incubating 250 mM. NAD^+ has been shown to play not only a unique role in DNA damage response, it is also for protein deacetylation of central importance. It has been reported that PARPs and sirtuins regulate each other's levels and activities and have opposite effects on the same pathways regulating cellular response to stress [41]. Recently, Mouchiroud et al. (2013) reported in a *C. elegans* study that increasing NAD^+ levels extends lifespan through sir-2.1 (homology to human SIRT1) [38]. The reason for the Mn-induced increased NAD^+ levels and the potential role for sirtuins need to be clarified in future studies.

Mn-induced oxidative stress has been suggested to be an important underlying mechanism of Mn-induced neurotoxicity. Mn increases the formation of reactive oxygen/nitrogen species (RONS), directly promoting oxidant generation or indirectly inhibiting complex I–IV activity of the mitochondrial electron transfer chain enzymes as well as dysregulating cellular energy or disturbing the cellular oxidative defense systems [42, 43]. A major obstacle, however, in understanding the contribution of Mn to oxidative stress is the widely recognized methodological difficulty in quantifying oxidative stress/damage markers *in vivo*. Therefore, analyzed oxidative stress endpoints in *C. elegans* include the quantification of the GSH:GSSG ratio, energy related nucleotides (ATP, ADP, AMP, NAD^+, NADH), the mitochondrial membrane potential- and mitochondrial-derived RONS as well as the mitochondrial mass. Analogous to higher organisms [44, 45], in worms Mn increased the formation of GSSG and consequently reduced the GSH:GSSG ratio (Figure 5 A and B). Multiple studies upon subcellular Mn distribution pointed out to mitochondrial accumulation of Mn, resulting in mitochondrial dysfunction [32, 46, 47]. This is corroborated by the Mn-induced mitochondrial mass reduction we observed herein, as well as the disturbed mitochondrial membrane potential- and Mn-induced mitochondrial-derived RONS (Figure 3C). As a consequence of the Mn-induced mitochondrial dysfunction, energy related nucleotides as the NAD^+/NADH ratio as well as ATP are affected [29]. Also, in this study Mn exposure resulted in depletion of ATP levels and increased NAD^+/NADH ratio was observed (Figure 4A and C). Such a decline in the cellular energy metabolism has also been reported to be disturbed in neurodegenerative diseases [48]. Consistent with Mn-induced oxidative stress SKN-1 (homolog of the mammalian Nrf2) overexpression afforded protection, while deletion rendered the worm more vulnerable to Mn toxicity [49].

The current study assessed further the functional roles of the PARP1 and PARP2 orthologues within Mn-induced oxidative stress in *C. elegans*. In general, the role of PARP1 in oxidative stress remains controversial. While some studies reported that a genetic deletion of PARP1 or PARP inhibition is protective against oxidative stress [16, 50–52], others show an increased oxidative stress upon PARP inhibition [53, 54]. Regarding the Mn-induced

lethality in the present study, pme-1 as well as pme-2 mutants showed dose-response survival curves indistinguishable from WT worms (Figure 1). The data of the GSSG level and GSH/GSSG ratio indicate a slightly attenuated Mn-induced oxidative stress in pme-2 deletion mutants in comparison to the pme-1 deletion mutants. Possible counter-regulating mechanisms need to be investigated in future studies as for example the consequence of loss of pme-2 on antioxidative defense mechanisms, as daf-16 or skn-1. PARP inhibition represents an attractive target for treating mitochondrial dysfunction [55]. The data of the present study clearly indicate that in the background of pme-1 and pme-2 deletion Mn-induced mitochondrial-derived RONS are diminished (Figure 5C). Additionally, the mitochondrial mass was less affected by Mn in the pme-1 deletion mutants (Figure 5D). With respect to the consequences of PARP inhibition, in the case pme-1 deletion mutants exposed to 100 mM Mn, we can neither point out an obvious higher sensitivity (even it is slightly indicated in the GSH/GSSG ratio (Figure 5B) nor a lower sensitivity towards Mn-induced oxidative stress. Further studies, especially with PARP inhibitors before Mn exposure need to be performed to shed more light on this issue, as to date the knowledge is rather limited.

Taken together, short term Mn exposure at the LD50 dose resulted in a PAR-induction in pme-1 deletion mutants due to induced pme-2 gene expression. This counter-regulating mechanisms needs to be critically taken into account, using the pme-1 mutant as model to simulate low PAR levels in order to study for example consequences of PAR inhibition. For this purpose the PAR level in the nematode needs to be monitored by quantifying the PAR level after exposition. The underlying mechanisms for the counter-regulating effect of the pme-1 mutants needs to be clarified in further studies which will further improve our understanding of PARylation-dependent mechanisms in the nematode *C. elegans*. Furthermore, Mn-induced oxidative stress, which represents a possible mode of action of Mn-induced toxicity, was not exacerbated in pme-1 or pme-2 deletion mutants. However, consequences of PAR inhibition on Mn-induced oxidative stress need to be further characterized. Whether PARP1 inhibition affects brain physiology and physiopathology in the context of manganism needs to be investigated in future studies.

Supplementary Material

Refer to Web version on PubMed Central for supplementary material.

Acknowledgements

We thank the German Research Foundation (DFG) for the financial support of BO 4103/2–1, INST 38/537–1, as well as the DFG Research Unit TraceAge (FOR 2558) and the Konstanz Research School Chemical Biology (KoRS-CB, GSC 218). We thank for the European Regional Development Fund (EFRE). We would also like to thank the Caenorhabditis Genetics Center (CGC), which is funded by the NIH Office of Research Infrastructure Programs (P40 OD010440), for providing the *C. elegans* strains used in this work. MA was supported in part by grants from the National Institute of Environmental Health Sciences (NIEHS), R01 ES10563 R01 ES07331.

References

[1]. Bjorklund G, Stejskal V, Urbina MA, Dadar M, Chirumbolo S, Mutter J, Metals and Parkinson's Disease: Mechanisms and Biochemical Processes, Curr Med Chem 25(19) (2018) 2198–2214. [PubMed: 29189118]

[2]. Pfalzer AC, Bowman AB, Relationships Between Essential Manganese Biology and Manganese Toxicity in Neurological Disease, Curr Environ Health Rep 4(2) (2017) 223–228. [PubMed: 28417441]

[3]. Chen P, Bornhorst J, Aschner M, Manganese metabolism in humans, Front Biosci (Landmark Ed) 23 (2018) 1655–1679. [PubMed: 29293455]

[4]. Koller WC, Lyons KE, Truly W, Effect of levodopa treatment for parkinsonism in welders: A double-blind study, Neurology 62(5) (2004) 730–3. [PubMed: 15007122]

[5]. Guilarte TR, Manganese neurotoxicity: new perspectives from behavioral, neuroimaging, and neuropathological studies in humans and non-human primates, Front Aging Neurosci 5 (2013) 23. [PubMed: 23805100]

[6]. Michalke B, Fernsebner K, New insights into manganese toxicity and speciation, J Trace Elem Med Biol 28(2) (2014) 106–16. [PubMed: 24200516]

[7]. Rahman SM, Kippler M, Tofail F, Bolte S, Hamadani JD, Vahter M, Manganese in Drinking Water and Cognitive Abilities and Behavior at 10 Years of Age: A Prospective Cohort Study, Environ Health Perspect 125(5) (2017) 057003. [PubMed: 28564632]

[8]. Haynes EN, Sucharew H, Kuhnell P, Alden J, Barnas M, Wright RO, Parsons PJ, Aldous KM, Praamsma ML, Beidler C, Dietrich KN, Manganese Exposure and Neurocognitive Outcomes in Rural School-Age Children: The Communities Actively Researching Exposure Study (Ohio, USA), Environ Health Perspect 123(10) (2015) 1066–71. [PubMed: 25902278]

[9]. Peres TV, Schettinger MR, Chen P, Carvalho F, Avila DS, Bowman AB, Aschner M, "Manganese-induced neurotoxicity: a review of its behavioral consequences and neuroprotective strategies", BMC Pharmacol Toxicol 17(1) (2016) 57. [PubMed: 27814772]

[10]. Bornhorst J, Ebert F, Hartwig A, Michalke B, Schwerdtle T, Manganese inhibits poly(ADP-ribosyl)ation in human cells: a possible mechanism behind manganese-induced toxicity?, J Environ Monit 12(11) (2010) 2062–9. [PubMed: 20820627]

[11]. Bornhorst J, Meyer S, Weber T, Boker C, Marschall T, Mangerich A, Beneke S, Burkle A, Schwerdtle T, Molecular mechanisms of Mn induced neurotoxicity: RONS generation, genotoxicity, and DNA-damage response, Mol Nutr Food Res 57(7) (2013) 1255–69. [PubMed: 23495240]

[12]. Henning RJ, Bourgeois M, Harbison RD, Poly(ADP-ribose) Polymerase (PARP) and PARP Inhibitors: Mechanisms of Action and Role in Cardiovascular Disorders, Cardiovascular toxicology 18(6) (2018) 493–506. [PubMed: 29968072]

[13]. Schuhwerk H, Atteya R, Siniuk K, Wang ZQ, PARPing for balance in the homeostasis of poly(ADP-ribosyl)ation, Seminars in cell & developmental biology 63 (2017) 81–91. [PubMed: 27664469]

[14]. Burkle A, Poly(ADP-ribose). The most elaborate metabolite of NAD+, The FEBS journal 272(18) (2005) 4576–89. [PubMed: 16156780]

[15]. Vida A, Marton J, Miko E, Bai P, Metabolic roles of poly(ADP-ribose) polymerases, Seminars in cell & developmental biology 63 (2017) 135–143. [PubMed: 28013023]

[16]. Narne P, Pandey V, Simhadri PK, Phanithi PB, Poly(ADP-ribose)polymerase-1 hyperactivation in neurodegenerative diseases: The death knell tolls for neurons, Seminars in cell & developmental biology 63 (2017) 154–166. [PubMed: 27867042]

[17]. Kam TI, Mao X, Park H, Chou SC, Karuppagounder SS, Umanah GE, Yun SP, Brahmachari S, Panicker N, Chen R, Andrabi SA, Qi C, Poirier GG, Pletnikova O, Troncoso JC, Bekris LM, Leverenz JB, Pantelyat A, Ko HS, Rosenthal LS, Dawson TM, Dawson VL, Poly(ADP-ribose) drives pathologic alpha-synuclein neurodegeneration in Parkinson's disease, Science 362(6414) (2018).

[18]. Visochek L, Steingart RA, Vulih-Shultzman I, Klein R, Priel E, Gozes I, Cohen-Armon M, PolyADP-ribosylation is involved in neurotrophic activity, The Journal of neuroscience : the official journal of the Society for Neuroscience 25(32) (2005) 7420–8. [PubMed: 16093393]

[19]. Cohen-Armon M, Visochek L, Katzoff A, Levitan D, Susswein AJ, Klein R, Valbrun M, Schwartz JH, Long-term memory requires polyADP-ribosylation, Science 304(5678) (2004) 1820–2. [PubMed: 15205535]

[20]. Hernandez-Bonilla D, Schilmann A, Montes S, Rodriguez-Agudelo Y, Rodriguez-Dozal S, Solis-Vivanco R, Rios C, Riojas-Rodriguez H, Environmental exposure to manganese and motor function of children in Mexico, Neurotoxicology 32(5) (2011) 615–21. [PubMed: 21871921]

[21]. Menezes-Filho JA, Novaes Cde O, Moreira JC, Sarcinelli PN, Mergler D, Elevated manganese and cognitive performance in school-aged children and their mothers, Environ Res 111(1) (2011) 156–63. [PubMed: 20943219]

[22]. Bouchard MF, Sauve S, Barbeau B, Legrand M, Brodeur ME, Bouffard T, Limoges E, Bellinger DC, Mergler D, Intellectual impairment in school-age children exposed to manganese from drinking water, Environ Health Perspect 119(1) (2011) 138–43. [PubMed: 20855239]

[23]. Leung MC, Williams PL, Benedetto A, Au C, Helmcke KJ, Aschner M, Meyer JN, Caenorhabditis elegans: an emerging model in biomedical and environmental toxicology, Toxicol Sci 106(1) (2008) 5–28. [PubMed: 18566021]

[24]. Brenner S, The genetics of Caenorhabditis elegans, Genetics 77(1) (1974) 71–94. [PubMed: 4366476]

[25]. Henze A, Homann T, Rohn I, Aschner M, Link CD, Kleuser B, Schweigert FJ, Schwerdtle T, Bornhorst J, Caenorhabditis elegans as a model system to study posttranslational modifications of human transthyretin, Sci Rep 6 (2016) 37346. [PubMed: 27869126]

[26]. Martello R, Mangerich A, Sass S, Dedon PC, Burkle A, Quantification of cellular poly(ADP-ribosyl)ation by stable isotope dilution mass spectrometry reveals tissue- and drug-dependent stress response dynamics, ACS Chem Biol 8(7) (2013) 1567–75. [PubMed: 23631432]

[27]. Zubel T, Martello R, Burkle A, Mangerich A, Quantitation of Poly(ADP-Ribose) by Isotope Dilution Mass Spectrometry, Methods Mol Biol 1608 (2017) 3–18. [PubMed: 28695499]

[28]. Bornhorst J, Chakraborty S, Meyer S, Lohren H, Brinkhaus SG, Knight AL, Caldwell KA, Caldwell GA, Karst U, Schwerdtle T, Bowman A, Aschner M, The effects of pdr1, djr1.1 and pink1 loss in manganese-induced toxicity and the role of alpha-synuclein in C. elegans, Metallomics 6(3) (2014) 476–90. [PubMed: 24452053]

[29]. Bornhorst J, Ebert F, Lohren H, Humpf HU, Karst U, Schwerdtle T, Effects of manganese and arsenic species on the level of energy related nucleotides in human cells, Metallomics 4(3) (2012) 297–306. [PubMed: 22266671]

[30]. Nowotny K, Castro JP, Hugo M, Braune S, Weber D, Pignitter M, Somoza V, Bornhorst J, Schwerdtle T, Grune T, Oxidants produced by methylglyoxal-modified collagen trigger ER stress and apoptosis in skin fibroblasts, Free Radic Biol Med 120 (2018) 102–113. [PubMed: 29550330]

[31]. Caito SW, Aschner M, NAD+ Supplementation Attenuates Methylmercury Dopaminergic and Mitochondrial Toxicity in Caenorhabditis Elegans, Toxicol Sci 151(1) (2016) 139–49. [PubMed: 26865665]

[32]. Milatovic D, Zaja-Milatovic S, Gupta RC, Yu Y, Aschner M, Oxidative damage and neurodegeneration in manganese-induced neurotoxicity, Toxicol Appl Pharmacol 240(2) (2009) 219–25. [PubMed: 19607852]

[33]. Edifizi D, Schumacher B, Genome Instability in Development and Aging: Insights from Nucleotide Excision Repair in Humans, Mice, and Worms, Biomolecules 5(3) (2015) 1855–69. [PubMed: 26287260]

[34]. Spagnolo L, Barbeau J, Curtin NJ, Morris EP, Pearl LH, Visualization of a DNA-PK/PARP1 complex, Nucleic acids research 40(9) (2012) 4168–77. [PubMed: 22223246]

[35]. Asagoshi K, Lehmann W, Braithwaite EK, Santana-Santos L, Prasad R, Freedman JH, Van Houten B, Wilson SH, Single-nucleotide base excision repair DNA polymerase activity in C. elegans in the absence of DNA polymerase beta, Nucleic acids research 40(2) (2012) 670–81. [PubMed: 21917855]

[36]. Gagnon SN, Hengartner MO, Desnoyers S, The genes pme-1 and pme-2 encode two poly(ADP-ribose) polymerases in Caenorhabditis elegans, The Biochemical journal 368(Pt 1) (2002) 263–71. [PubMed: 12145714]

[37]. Dequen F, Gagnon SN, Desnoyers S, Ionizing radiations in Caenorhabditis elegans induce poly(ADP-ribosyl)ation, a conserved DNA-damage response essential for survival, DNA repair 4(7) (2005) 814–25. [PubMed: 15923155]

[38]. Mouchiroud L, Houtkooper RH, Moullan N, Katsyuba E, Ryu D, Canto C, Mottis A, Jo YS, Viswanathan M, Schoonjans K, Guarente L, Auwerx J, The NAD(+)/Sirtuin Pathway Modulates Longevity through Activation of Mitochondrial UPR and FOXO Signaling, Cell 154(2) (2013) 430–41. [PubMed: 23870130]

[39]. Chen Q, Kassab MA, Dantzer F, Yu X, PARP2 mediates branched poly ADP-ribosylation in response to DNA damage, Nature communications 9(1) (2018) 3233.

[40]. Wang W, McReynolds MR, Goncalves JF, Shu M, Dhondt I, Braeckman BP, Lange SE, Kho K, Detwiler AC, Pacella MJ, Hanna-Rose W, Comparative Metabolomic Profiling Reveals That Dysregulated Glycolysis Stemming from Lack of Salvage NAD+ Biosynthesis Impairs Reproductive Development in Caenorhabditis elegans, J Biol Chem 290(43) (2015) 26163–79. [PubMed: 26350462]

[41]. Canto C, Auwerx J, Interference between PARPs and SIRT1: a novel approach to healthy ageing?, Aging (Albany NY) 3(5) (2011) 543–7. [PubMed: 21566260]

[42]. Zhang S, Zhou Z, Fu J, Effect of manganese chloride exposure on liver and brain mitochondria function in rats, Environ Res 93(2) (2003) 149–57. [PubMed: 12963399]

[43]. Chtourou Y, Trabelsi K, Fetoui H, Mkannez G, Kallel H, Zeghal N, Manganese induces oxidative stress, redox state unbalance and disrupts membrane bound ATPases on murine neuroblastoma cells in vitro: protective role of silymarin, Neurochem Res 36(8) (2011) 1546–57. [PubMed: 21533646]

[44]. Gawlik M, Gawlik MB, Smaga I, Filip M, Manganese neurotoxicity and protective effects of resveratrol and quercetin in preclinical research, Pharmacol Rep 69(2) (2017) 322–330. [PubMed: 28183032]

[45]. Fernsebner K, Zorn J, Kanawati B, Walker A, Michalke B, Manganese leads to an increase in markers of oxidative stress as well as to a shift in the ratio of Fe(II)/(III) in rat brain tissue, Metallomics 6(4) (2014) 921–31. [PubMed: 24599255]

[46]. Fernandes J, Hao L, Bijli KM, Chandler JD, Orr M, Hu X, Jones DP, Go YM, From the Cover: Manganese Stimulates Mitochondrial H2O2 Production in SH-SY5Y Human Neuroblastoma Cells Over Physiologic as well as Toxicologic Range, Toxicol Sci 155(1) (2017) 213–223. [PubMed: 27701121]

[47]. Sarkar S, Malovic E, Harischandra DS, Ngwa HA, Ghosh A, Hogan C, Rokad D, Zenitsky G, Jin H, Anantharam V, Kanthasamy AG, Kanthasamy A, Manganese exposure induces neuroinflammation by impairing mitochondrial dynamics in astrocytes, Neurotoxicology 64 (2018) 204–218. [PubMed: 28539244]

[48]. Guarente L, Franklin H Epstein Lecture: Sirtuins, aging, and medicine, N Engl J Med 364(23) (2011) 2235–44. [PubMed: 21651395]

[49]. Benedetto A, Au C, Avila DS, Milatovic D, Aschner M, Extracellular dopamine potentiates mn-induced oxidative stress, lifespan reduction, and dopaminergic neurodegeneration in a BLI-3-dependent manner in Caenorhabditis elegans, PLoS Genet 6(8) (2010).

[50]. Hegedus C, Virag L, Inputs and outputs of poly(ADP-ribosyl)ation: Relevance to oxidative stress, Redox Biol 2 (2014) 978–82. [PubMed: 25460733]

[51]. Hans CP, Feng Y, Naura AS, Zerfaoui M, Rezk BM, Xia H, Kaye AD, Matrougui K, Lazartigues E, Boulares AH, Protective effects of PARP-1 knockout on dyslipidemia-induced autonomic and vascular dysfunction in ApoE mice: effects on eNOS and oxidative stress, PLoS One 4(10) (2009) e7430. [PubMed: 19823587]

[52]. Wang C, Zhang F, Wang L, Zhang Y, Li X, Huang K, Du M, Liu F, Huang S, Guan Y, Huang D, Huang K, Poly(ADP-ribose) polymerase 1 promotes oxidative-stress-induced liver cell death via suppressing farnesoid X receptor alpha, Mol Cell Biol 33(22) (2013) 4492–503. [PubMed: 24043304]

[53]. Smith AJ, Ball SS, Bowater RP, Wormstone IM, PARP-1 inhibition influences the oxidative stress response of the human lens, Redox Biol 8 (2016) 354–62. [PubMed: 26990173]

[54]. Hou D, Liu Z, Xu X, Liu Q, Zhang X, Kong B, Wei JJ, Gong Y, Shao C, Increased oxidative stress mediates the antitumor effect of PARP inhibition in ovarian cancer, Redox Biol 17 (2018) 99–111. [PubMed: 29684820]

[55]. Martire S, Mosca L, d'Erme M, PARP-1 involvement in neurodegeneration: A focus on Alzheimer's and Parkinson's diseases, Mech Ageing Dev 146–148 (2015) 53–64.

Highlights:

- Highly sensitive LC-MS/MS method to quantify poly(ADP-ribosyl)ation in *C. elegans*
- Characterizing worms defective in pme-1 or pme-2 (orthologues of PARP1 and PARP2)
- pme-1 (orthologue of PARP1) holding the major worm PARP activity
- Toxic doses of Mn led to PAR-induction in pme-1-deficient *C. elegans*
- Mn-induced oxidative stress in pme-1 or pme-2 deletion mutants

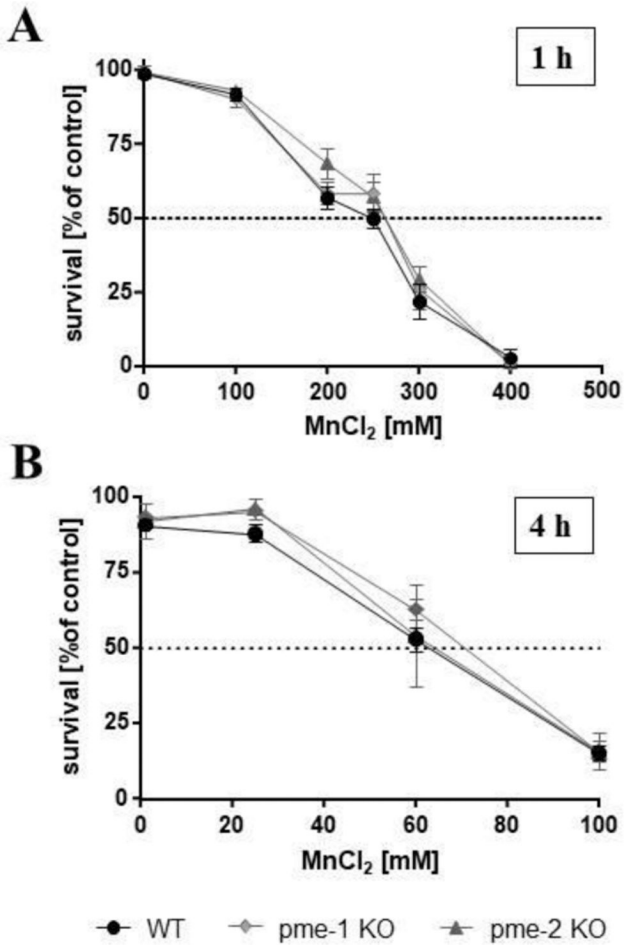

Figure 1:

Dose–response survival curves of L4 stage worms following 1 h [A] or 4 h [B] Mn exposure. Data are expressed as means ± SEM of at least four independent experiments.

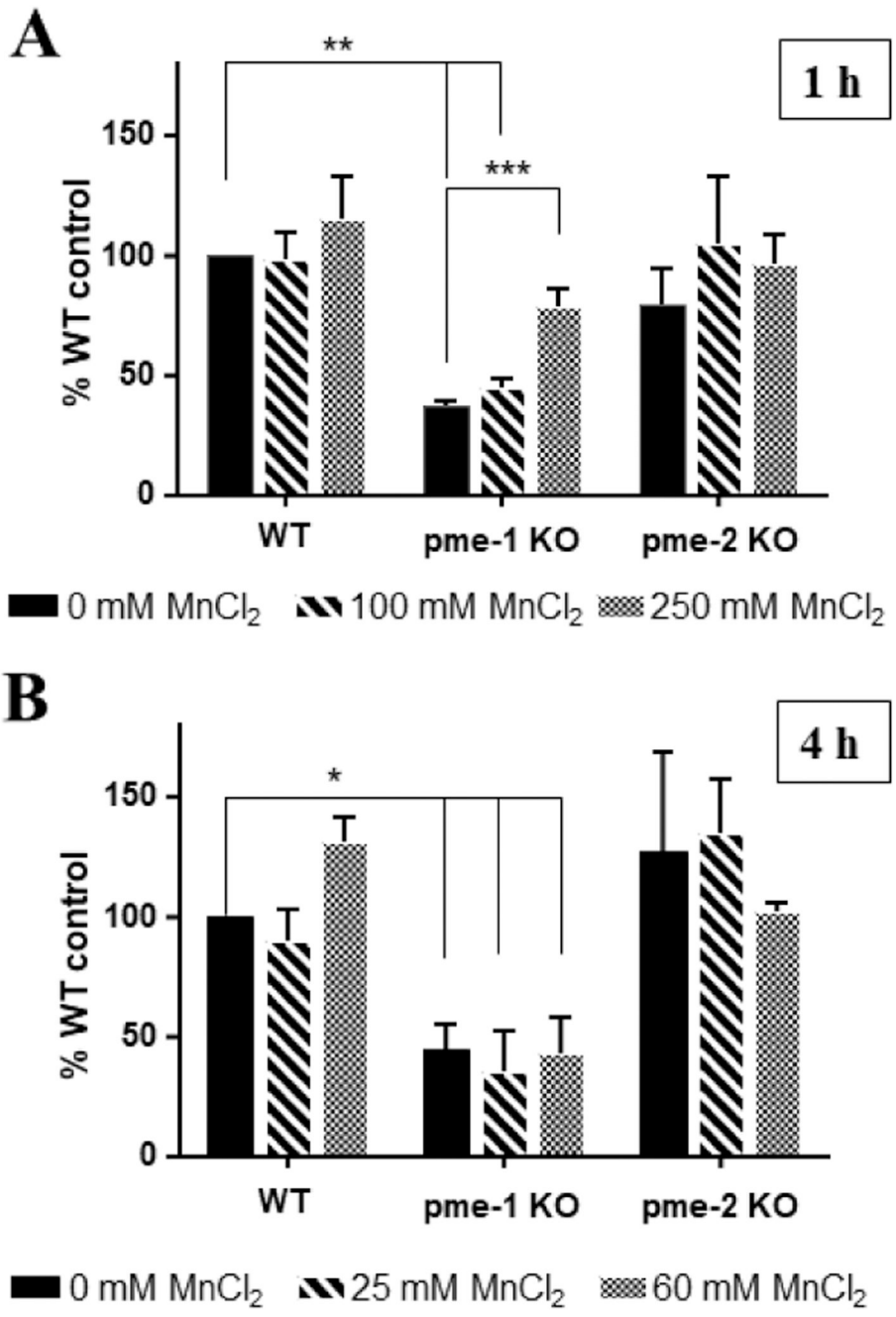

Figure 2:

Impact of Mn on PAR levels in worms analyzed by isotope-dilution liquid chromatography-tandem mass spectrometry (LC-MS/MS) [A, B]. [A] L4 worms were treated with 0 mM (control), 100 mM (subtoxic), 250 mM (LD50) $MnCl_2$ for 1 h. [B] L4 worms were treated with 0 mM (control), 25 mM (subtoxic) and 60 mM (LD50) $MnCl_2$ for 4 h. Data are expressed as means of at least 4 independent determinations + SEM normalized to WT worms (PAR level). *** $p < 0.001$, ** $p < 0.01$, * $p < 0.05$ versus WT controls.

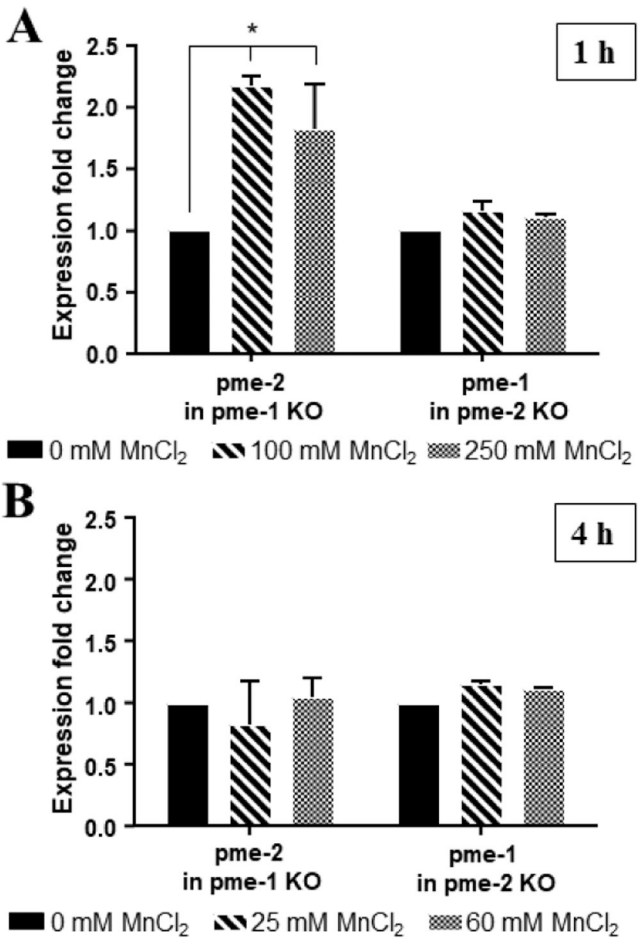

Figure 3:

Impact of Mn on the gene expression of pme-2 in the pme-1 deletion mutant or pme-1 in the pme-2 deletion mutant [A, B]. [A] L4 worms were treated with 0 mM (control), 100 mM (subtoxic), 250 mM (LD50) $MnCl_2$ for 1 h. [B] L4 worms were treated with 0 mM (control), 25 mM (subtoxic) and 60 mM (LD50) $MnCl_2$ for 4 h. Data are expressed as means of at least 4 independent determinations + SEM normalized to the respective control (gene expression). * $p < 0.05$ versus WT controls.

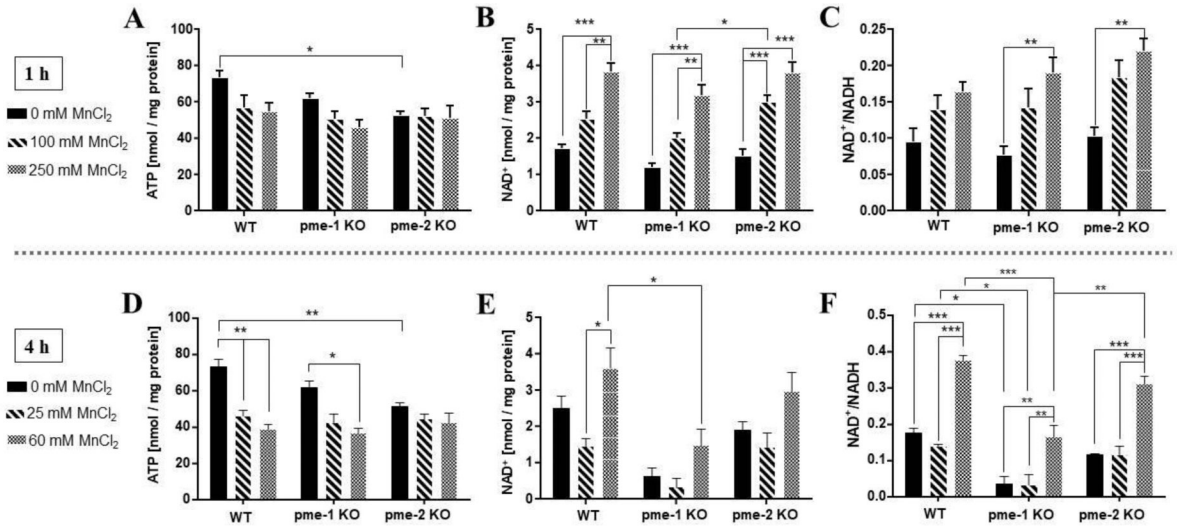

Figure 4:

ATP [A, D] and NAD+ [B, E] level as well as the NAD+/NADH ratio [C, F] following Mn exposure. [A – C] L4 worms were treated with 0 mM (control), 100 mM (subtoxic), 250 mM (LD50) $MnCl_2$ for 1 h. [D – F] L4 worms were treated with 0 mM (control), 25 mM (subtoxic) and 60 mM (LD50) $MnCl_2$ for 4 h. Data are expressed as means of at least 4 independent determinations + SEM normalized to the respective control. *** $p < 0.001$, ** $p < 0.01$, * $p < 0.05$

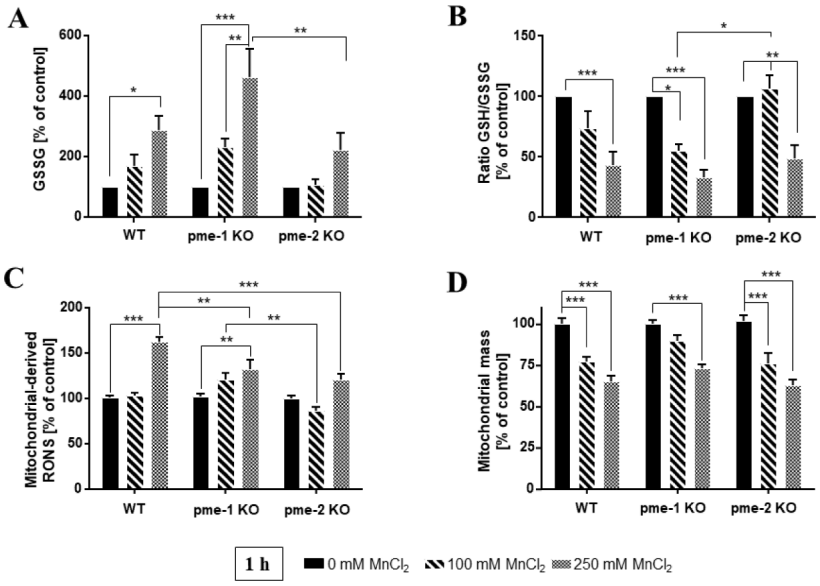

Figure 5:

Impact of Mn on the GSSG level and GSH/GSSG ratio quantified by isotope-dilution liquid chromatography-tandem mass spectrometry [A, B] following 1 h Mn exposure. [C] Mn-induced mitochondrial derived RONS stained with MitoTracker® Red CM-H2XROS and treated with Mn for 1 h. [D] Mitochondrial mass stained with MitoTracker® Green following 1 h Mn exposure. Data are expressed as means of at least 4 independent determinations + SEM normalized to the respective control. *** $p < 0.001$, ** $p < 0.01$, * $p < 0.05$